

# Current modulation at nano-scale level: A theoretical study

Santanu K. Maiti<sup>1,2</sup>

<sup>1</sup>*Theoretical Condensed Matter Physics Division,*

*Saha Institute of Nuclear Physics, 1/AF, Bidhannagar, Kolkata-700 064, India*

<sup>2</sup>*Department of Physics, Narasinha Dutt College, 129 Belilious Road, Howrah-711 101, India*

We explore the possibilities of current modulation at nano-scale level using mesoscopic rings. A single mesoscopic ring or an array of such rings is used for current modulation where each ring is threaded by a time varying magnetic flux  $\phi$  which plays the central role in the modulation action. Within a tight-binding framework, all the calculations are done based on the Green's function formalism. We present numerical results for the two-terminal conductance and current which support the essential features of current modulation. The analysis may be helpful in fabricating mesoscopic or nano-scale electronic devices.

PACS numbers: 73.63.-b, 73.63.Rt, 81.07.Nb

## I. INTRODUCTION

Electron transport in low-dimensional systems has drawn much attention in the field of theoretical as well as experimental research due to flourishing development in nanotechnology and nano-scale device modeling. Low-dimensional model quantum systems are the basic building blocks for future generation of nano-electronic devices. Several exotic features are observed in this length scale owing to the effect of quantum interference. This effect is generally observed in samples with size much smaller or comparable to phase coherence length  $L_\phi$ , while the effect disappears for larger systems. A normal metal mesoscopic ring is a very good example to study the effect of quantum interference. Current trend of fabricating nano-scale devices has resulted much interest in characterization of ring type nanostructures. There are several methods for preparation of mesoscopic rings. For instance, gold rings can be designed using templates of suitable structure in combination with metal deposition through ion beam etching [1, 2]. In a recent experiment, Yan *et al.* have proposed how gold rings can be prepared by selective wetting of porous templates using polymer membranes [3]. With such rings we can fabricate nano-scale electronic circuits which can be utilized for the operation of current modulation. To explore this phenomenon the ring is coupled to two electrodes, to form an electrode-ring-electrode bridge, where the ring is penetrated by a time varying magnetic flux  $\phi$ . Electron transport through a molecular bridge system was first studied theoretically by Aviram and Ratner [4] during 1970's. Following this pioneering work, several experiments have been done using different bridge systems to reveal the actual mechanism of electron transport. Though, to date a lot of theoretical [5–16] as well as experimental works [17–20] on two-terminal electron transport have been done addressing several important issues, yet the complete knowledge of conduction mechanism in nano-scale systems is still unclear to us. Transport properties are characterized by several significant factors like quantization of energy levels, quantum interference effect, ring-to-electrode interface geometry, etc.

Furthermore, electron transport in the ring can also be modulated in other way by tuning the magnetic flux, the so-called Aharonov-Bohm (AB) flux, penetrated by the ring.

Aim of the present paper is to illustrate the possibilities of current modulation at nano-scale level using simple mesoscopic rings. To achieve current modulation we design an electronic circuit using a single mesoscopic ring or a cluster of such rings, where each ring is penetrated by a time varying magnetic flux  $\phi$  which plays the central role for the modulation action. For a constant DC voltage, current through the circuit shows oscillatory behavior as a function of time  $t$  depending on the phase of the magnetic flux  $\phi$  passing through the ring. Therefore, current modulation can be achieved simply by tuning the phase of magnetic flux  $\phi$  threaded by the ring. Within a tight-binding framework, a simple parametric approach [21–29] is given and all the calculations are done through single particle Green's function technique to reveal the electron transport. Here we present numerical results for the two-terminal conductance and current which clearly describe the essential features of current modulation. Our exact analysis may be helpful for designing mesoscopic or nano-scale electronic devices. To the best of our knowledge the modulation action using such simple mesoscopic rings has not been addressed earlier in the literature.

The scheme of the present paper is as follows. With the brief introduction (Section I), in Section II, we describe the model and theoretical formulations for our calculations. Section III presents the significant results, and finally, we conclude our results in Section IV.

## II. MODEL AND SYNOPSIS OF THE THEORETICAL FORMULATION

In the forthcoming two sub-sections we focus on two different circuit configurations, for our illustrative purposes, those are used for current modulation. Here we try to illustrate how a single mesoscopic ring or two such rings, where each ring is penetrated by a time varying magnetic flux  $\phi$ , under a DC bias voltage can support an

oscillating output current. A single mesoscopic ring can provide an oscillating current with a particular frequency, while in the case of two rings, oscillating currents with other frequencies can be obtained. These ideas may be generalized further to produce oscillating currents with other frequencies by considering more number of rings.

### A. Circuit configuration I

Let us start by referring to Fig. 1. A mesoscopic ring, penetrated by a time varying magnetic flux  $\phi$ , is attached symmetrically to two semi-infinite one-dimensional (1D) metallic electrodes, namely, source and drain. These two electrodes are directly coupled to the positive and negative terminals of a battery, a source of constant voltage. The time varying magnetic flux passing through the ring

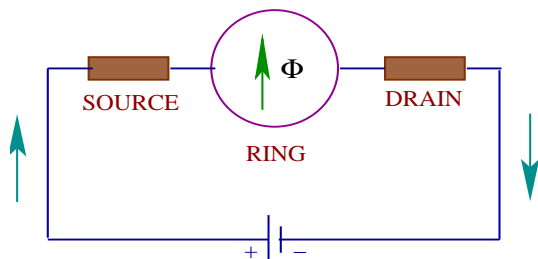


FIG. 1: (Color online). Actual scheme of connection with the battery where a mesoscopic ring, subject to a time varying magnetic flux  $\phi$ , is attached symmetrically to source and drain. The blue arrow indicates current direction in the circuit.

can be expressed mathematically in the form,

$$\phi(t) = \frac{\phi_0}{2} \sin(\omega t) \quad (1)$$

where,  $\phi_0 = ch/e$  is the elementary flux-quantum,  $\omega$  corresponds to the angular frequency and  $t$  represents the time. This electronic circuit provides an oscillating current in the output though a constant DC input signal is applied which we will describe in the forthcoming section. The frequency of the current is identical to that of the applied flux  $\phi(t)$ .

### B. Circuit configuration II

In Fig. 2 two such mesoscopic rings those are directly coupled to each other, penetrated by time varying magnetic fluxes  $\phi_1$  and  $\phi_2$  are attached symmetrically to the electrodes, viz, source and drain. A DC voltage source is connected to these two electrodes. The time varying magnetic fluxes are expressed mathematically as,

$$\phi_1(t) = \frac{\phi_0}{2} \sin(\omega t) \quad (2)$$

$$\phi_2(t) = \frac{\phi_0}{2} \sin(\omega t + \delta) \quad (3)$$

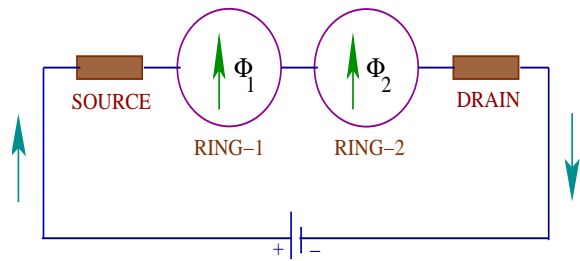


FIG. 2: (Color online). Actual scheme of connection with the battery where two mesoscopic rings, subject to time varying magnetic fluxes  $\phi_1$  and  $\phi_2$  are attached symmetrically to source and drain. The blue arrow indicates current direction in the circuit.

where,  $\delta$  refers to constant phase difference between the two fluxes  $\phi_1$  and  $\phi_2$ . Using this circuit configuration also oscillating current in the output can be achieved, but in this case the frequency of the current gets modified depending on the phase shift  $\delta$ .

### C. Theoretical formulation

In this sub-section we will describe the basic theoretical formulation for calculation of conductance and current through a single mesoscopic ring, penetrated by a magnetic flux  $\phi$ , attached to two source and drain. This similar theory is also used to study electron transport in an array of mesoscopic rings.

Using Landauer conductance formula [30, 31] we determine two-terminal conductance ( $g$ ) of the mesoscopic ring. At much low temperatures and bias voltage it ( $g$ ) can be written in the form,

$$g = \frac{2e^2}{h} T \quad (4)$$

where,  $T$  corresponds to the transmission probability of an electron across the ring. In terms of the Green's function of the ring and its coupling to two electrodes, the transmission probability can be expressed as [30, 31],

$$T = \text{Tr} [\Gamma_1 G_R^r \Gamma_2 G_R^a] \quad (5)$$

where,  $\Gamma_S$  and  $\Gamma_D$  describe the coupling of the ring to the source and drain, respectively. Here,  $G_R^r$  and  $G_R^a$  are the retarded and advanced Green's functions, respectively, of the ring considering the effects of the electrodes. Now, for the full system i.e., the mesoscopic ring, source and drain, the Green's function is expressed as,

$$G = (E - H)^{-1} \quad (6)$$

where,  $E$  is the energy of the source electron. Evaluation of this Green's function needs the inversion of an infinite matrix, which is really a difficult task, since the full system consists of the finite size ring and two semi-infinite 1D electrodes. However, the full system can be

partitioned into sub-matrices corresponding to the individual sub-systems and the effective Green's function for the ring can be written in the form [30, 31],

$$G_R = (E - H_R - \Sigma_S - \Sigma_D)^{-1} \quad (7)$$

where,  $H_R$  describes the Hamiltonian of the ring. Within the non-interacting picture, the tight-binding Hamiltonian of the ring can be expressed like,

$$H_R = \sum_i \epsilon_i c_i^\dagger c_i + \sum_{\langle ij \rangle} v \left( c_i^\dagger c_j e^{i\theta} + c_j^\dagger c_i e^{-i\theta} \right) \quad (8)$$

where,  $\epsilon_i$  and  $v$  correspond to the site energy and nearest-neighbor hopping strength, respectively.  $c_i^\dagger$  ( $c_i$ ) is the creation (annihilation) operator of an electron at the site  $i$  and  $\theta = 2\pi\phi/N\phi_0$  is the phase factor due to the flux  $\phi$  enclosed by the ring consists of  $N$  atomic sites. A similar kind of tight-binding Hamiltonian is also used, except the phase factor  $\theta$ , to describe the electrodes where the Hamiltonian is parametrized by constant on-site potential  $\epsilon'$  and nearest-neighbor hopping integral  $t'$ . The hopping integral between the ring and source is  $\tau_S$ , while it is  $\tau_D$  between the ring and drain. In Eq. (7),  $\Sigma_S$  and  $\Sigma_D$  are the self-energies due to the coupling of the ring to the source and drain, respectively, where all the information of the coupling are included into these self-energies.

To determine current, passing through the mesoscopic ring, we use the expression [30, 31],

$$I(V) = \frac{2e}{h} \int_{-\infty}^{\infty} (f_S - f_D) T(E) dE \quad (9)$$

where,  $f_{S(D)} = f(E - \mu_{S(D)})$  gives the Fermi distribution function with the electrochemical potential  $\mu_{S(D)} = E_F \pm eV/2$  and  $E_F$  is the equilibrium Fermi energy. For the sake of simplicity, we take the unit  $c = e = h = 1$  in our present calculations.

### III. NUMERICAL RESULTS AND DISCUSSION

To illustrate the numerical results, we begin our discussion by mentioning the values of different parameters used for our calculations. In the mesoscopic ring, the on-site energy  $\epsilon_i$  is fixed to 0 for all the atomic sites  $i$  and nearest-neighbor hopping strength  $v$  is set to 3. While, for the side-attached electrodes the on-site energy ( $\epsilon'$ ) and nearest-neighbor hopping strength ( $t'$ ) are chosen as 0 and 4, respectively. The hopping strengths  $\tau_S$  and  $\tau_D$  are set as  $\tau_S = \tau_D = 2.5$ . The equilibrium Fermi energy  $E_F$  is fixed at 0.

#### A. Responses in circuit configuration I

The modulation action for the circuit configuration I is clearly illustrated in Fig. 3, where we compute all the

results considering a ring with  $N = 20$ . The upper panel presents the time variation of magnetic flux with amplitude  $\phi_0/2$  whose mathematical form is given in Eq. (1). The variation of conductance  $g$  as a function of time  $t$  is illustrated in the middle panel. Here we determine the typical conductance for a particular energy  $E = 2.5$ . It shows that the conductance oscillates periodically as a function of  $\omega t$  exhibiting  $\pi$  periodicity and it gets the amplitude  $g_{max} = 2$ . This reveals that the transmission amplitude  $T$  becomes unity since we get the relation  $g = 2T$  from the Landauer conductance formula in our chosen unit  $c = e = h = 1$ . Now we try to justify the os-

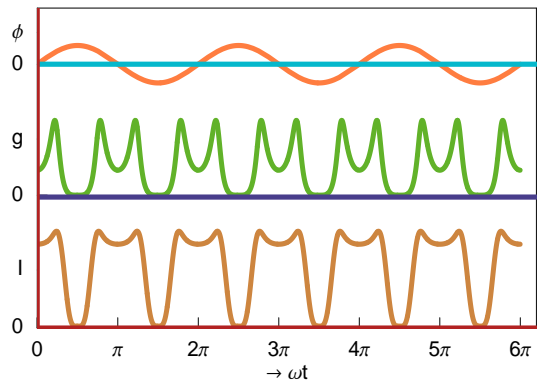


FIG. 3: (Color online). Responses in circuit configuration I. Upper, middle and lower panels describe the time dependences of flux  $\phi$ , conductance  $g$  and current  $I$  as a function of time  $t$ . Conductance is calculated at the energy  $E = 2.5$  and current is determined at the typical bias voltage  $V = 2.5$ . The ring size is fixed at  $N = 20$ . The amplitudes are:  $\phi_{max} = 0.5$ ,  $g_{max} = 2$  and  $I_{max} = 2.54$ .

cillating behavior of conductance with time  $t$ . The probability amplitude of getting an electron from the source to drain across the ring depends on the quantum interference effect of the electronic waves passing through the upper and lower arms of the ring. For a symmetrically connected ring (upper and lower arms are identical to each other), penetrated by a magnetic flux  $\phi$ , the probability amplitude of getting an electron across the ring becomes exactly zero ( $T = 0$ ) for the typical flux,  $\phi = \phi_0/2$ . This vanishing behavior of transmission probability can be shown very easily by simple mathematical calculation as follows.

For a symmetrically connected ring, the wave functions passing through the upper and lower arms of the ring are given by,

$$\begin{aligned} \psi_1 &= \psi_0 e^{-\gamma_1 \int \frac{i\epsilon}{\hbar c} \vec{A} \cdot d\vec{r}} \\ \psi_2 &= \psi_0 e^{-\gamma_2 \int \frac{i\epsilon}{\hbar c} \vec{A} \cdot d\vec{r}} \end{aligned} \quad (10)$$

where,  $\gamma_1$  and  $\gamma_2$  are used to indicate the two different paths of electron propagation along the two arms of the ring.  $\psi_0$  denotes the wave function in absence of magnetic flux  $\phi$  and it is same for both upper and lower arms as the

ring is symmetrically coupled to the electrodes.  $\vec{A}$  is the vector potential associated with the magnetic field  $\vec{B}$  by the relation  $\vec{B} = \vec{\nabla} \times \vec{A}$ . Hence the probability amplitude of finding the electron passing through the ring can be calculated as,

$$|\psi_1 + \psi_2|^2 = 2|\psi_0|^2 + 2|\psi_0|^2 \cos\left(\frac{2\pi\phi}{\phi_0}\right) \quad (11)$$

where,  $\phi = \oint \vec{A} \cdot d\vec{r} = \int \int \vec{B} \cdot d\vec{s}$  is the flux enclosed by the ring.

From Eq. (11) it is clearly observed that at  $\phi = \phi_0/2$  the transmission probability of an electron drops exactly to zero. On the other hand, for all other values of  $\phi$  i.e.,  $\phi \neq \phi_0/2$ , electron transmission through the ring takes place which provides non-zero value of conductance. Thus, for the particular cases when  $\phi(t)$  becomes maximum ( $+\phi_0/2$ ) or minimum ( $-\phi_0/2$ ), conductance drops to zero which is clearly shown from the conductance spectrum (middle panel of Fig. 3). Hence, changing the frequency of time dependent flux  $\phi(t)$ , periodicity in conductance can be regulated. To visualize the oscillatory action more prominently we present the variation of current as a function of  $\omega t$  in the lower panel of Fig. 3. The current  $I$  through the ring is obtained by integrating over the transmission function  $T$  (see Eq. (9)). Here we compute the current for the typical bias voltage  $V = 2.5$ . Following the conductance pattern, the oscillatory behavior of the current is clearly understood, and like the conductance spectrum current exhibits  $\pi$  periodicity providing the amplitude  $I_{max} = 2.54$ . All these characteristic features suggest that an oscillatory response in the output is obtained though the ring is subject to a DC bias voltage.

### B. Responses in circuit configuration II

Next, we concentrate on the responses obtained in the circuit configuration II. The results are illustrated in Fig. 4, where total number of atomic sites  $N$  in each ring is fixed at 8. In the upper panel, we plot the time dependent fluxes  $\phi_1(t)$  (orange line) and  $\phi_2(t)$  (magenta line) those pass through two different rings. A constant phase shift  $\delta$  exists between these two fluxes as mathematically expressed in Eqs. (2) and (3). Here we set  $\delta = \pi/2$ . In the middle panel, we describe the time dependence of conductance  $g$  with amplitude  $g_{max} = 1.9$ , where conductance is evaluated at the typical energy  $E = 2.5$ . Conductance shows the oscillatory behavior as a function of  $\omega t$  providing  $\pi/2$  periodicity. Thus, for this circuit configuration II, periodicity becomes exactly half compared to the circuit configuration I. The explanation of  $\pi/2$  periodicity is as follows. For this two ring system, the transmission probability depends on the combined effect of quantum interferences in the two rings. In ring-1,  $\phi_1(t)$  is sinusoidal in form as described mathematically in Eq. (2), while in ring-2, the variation of flux  $\phi_2(t)$  is the same

as in ring-1 with a phase shift  $\pi/2$ . Therefore, ring-1 and ring-2 enclose  $\phi_0/2$  flux alternatively in the interval  $\omega t = \pi/2$ , and accordingly, zero transmission probability is achieved at this interval. In the same footing, here we also describe the variation current  $I$  with time  $t$  (see lower panel of Fig. 4) to support the oscillatory action observed in this circuit configuration II. The current is computed at the typical bias voltage  $V = 4$ . The variation of current shows  $\pi/2$  periodicity with an amplitude  $I_{max} = 2$  and this periodic nature is well understood from the conductance spectrum. From these conductance and current

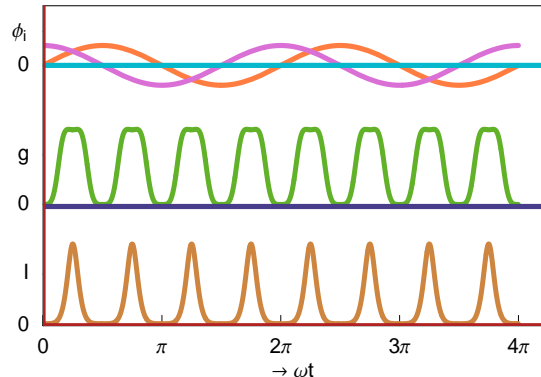


FIG. 4: (Color online). Responses in circuit configuration II. Upper, middle and lower panels describe the time dependences of two fluxes  $\phi_1$  (orange line) and  $\phi_2$  (magenta line), conductance  $g$  and current  $I$  as a function of time  $t$ . Conductance is calculated at the energy  $E = 2.5$  and current is determined at the typical bias voltage  $V = 4$ . In each ring, total number of atomic sites  $N$  is fixed at 8 and we choose  $\delta = \pi/2$ . The amplitudes are:  $\phi_{max} = 0.5$ ,  $g_{max} = 1.9$  and  $I_{max} = 2$ .

spectra it is manifested that in the two ring system which is subject to a DC bias voltage, the oscillatory response can be modulated very easily by tuning the phase difference  $\delta$  between two time varying magnetic fluxes.

Finally, we can say that extending this idea to an array of multi-ring system in which different rings subject to time varying magnetic fluxes in different phases, oscillatory responses can be achieved with  $\pi/n$  frequencies, where  $n$  corresponds to an integer. Our exact analysis may provide some significant insights in designing nano-electronic circuits.

## IV. CONCLUDING REMARKS

In a nutshell, we have addressed the possibilities of current modulation at nano-scale level using mesoscopic rings enclosing a time varying magnetic flux. We have shown that a single mesoscopic ring or two such rings, subject to a DC bias voltage, can support an oscillating output current. A single mesoscopic ring can exhibit an oscillating current with a particular frequency associated with the flux  $\phi(t)$ , while the frequency of the



current can be regulated in the case of two rings by tuning the phase difference  $\delta$  between the fluxes  $\phi_1(t)$  and  $\phi_2(t)$ . The whole modulation action is based on the central idea of quantum interference effect in presence of flux  $\phi$  in ring shaped geometries. We adopt a simple tight-binding framework to illustrate the model and all the calculations are done using single particle Green's function formalism. Our exact numerical results provide two-terminal conductance and current which clearly describe the essential features of current modulation. Our analysis can be used in designing tailor made nano-scale electronic devices.

Throughout our work, we have described all the essential features of current modulation for two different ring sizes. In circuit configuration I, we have chosen a ring with total number of atomic sites  $N = 20$ . On the other hand, in circuit configuration II, we have considered two identical rings, where each ring contains 8 atomic sites. In our model calculations, these typical numbers (20 or  $2 \times 8 = 16$ ) are chosen only for the sake of simplicity. Though the results presented here change numerically with the ring size ( $N$ ), but all the basic features remain

exactly invariant. To be more specific, it is important to note that, in real situation the experimentally achievable rings have typical diameters within the range 0.4-0.6  $\mu\text{m}$ . In such a small ring, unrealistically very high magnetic fields are required to produce a quantum flux. To overcome this situation, Hod *et al.* have studied extensively and proposed how to construct nanometer scale devices, based on Aharonov-Bohm interferometry, those can be operated in moderate magnetic fields [32–35].

In the present paper we have done all the calculations by ignoring the effects of the temperature, electron-electron correlation, etc. Due to these factors, any scattering process that appears in the mesoscopic ring would have influence on electronic phases, and, in consequences can disturb the quantum interference effects. Here we have assumed that, in our sample all these effects are too small, and accordingly, we have neglected all these factors in this particular study.

The importance of this article is mainly concerned with (i) the simplicity of the geometry and (ii) the smallness of the size.

- 
- [1] K. L. Hobbs, P. R. Larson, G. D. Lian, J. C. Keay, and M. B. Johnson, *Nano Lett.* **4**, 167 (2004).
- [2] D. H. Pearson, R. J. Tonucci, K. M. Bussmann, and E. A. Bolden, *Adv. Mater.* **11**, 769 (1999).
- [3] F. Yan and W. A. Geedel, *Nano Lett.* **4**, 1193 (2004).
- [4] A. Aviram and M. Ratner, *Chem. Phys. Lett.* **29**, 277 (1974).
- [5] M. Magoga and C. Joachim, *Phys. Rev. B* **59**, 16011 (1999).
- [6] J.-P. Launay and C. D. Coudret, in: A. Aviram and M. A. Ratner (Eds.), *Molecular Electronics*, New York Academy of Sciences, New York, (1998).
- [7] R. Baer and D. Neuhauser, *Chem. Phys.* **281**, 353 (2002).
- [8] R. Baer and D. Neuhauser, *J. Am. Chem. Soc.* **124**, 4200 (2002).
- [9] D. Walter, D. Neuhauser, and R. Baer, *Chem. Phys.* **299**, 139 (2004).
- [10] K. Tagami, L. Wang, and M. Tsukada, *Nano Lett.* **4**, 209 (2004).
- [11] R. H. Goldsmith, M. R. Wasielewski, and M. A. Ratner, *J. Phys. Chem. B* **110**, 20258 (2006).
- [12] W. Y. Cui, S. Z. Wu, G. Jin, X. Zhao, and Y. Q. Ma, *Eur. Phys. J. B* **59**, 47 (2007).
- [13] P. A. Orellana, M. L. Ladron de Guevara, M. Pacheco, and A. Latge, *Phys. Rev. B* **68**, 195321 (2003).
- [14] P. A. Orellana, F. Dominguez-Adame, I. Gomez, and M. L. Ladron de Guevara, *Phys. Rev. B* **67**, 085321 (2003).
- [15] B. T. Pickup and P. W. Fowler, *Chem. Phys. Lett.* **459**, 198 (2008).
- [16] P. Földi, B. Molnar, M. G. Benedict, and F. M. Peeters, *Phys. Rev. B* **71**, 033309 (2005).
- [17] J. Chen, M. A. Reed, A. M. Rawlett, and J. M. Tour, *Science* **286**, 1550 (1999).
- [18] M. A. Reed, C. Zhou, C. J. Muller, T. P. Burgin, and J. M. Tour, *Science* **278**, 252 (1997).
- [19] T. Dadoosh, Y. Gordin, R. Krahn, I. Khivrich, D. Mahalu, V. Frydman, J. Sperling, A. Yacoby, and I. Bar-Joseph, *Nature* **436**, 677 (2005).
- [20] C. M. Fischer, M. Burghard, S. Roth, and K. V. Klitzing, *Appl. Phys. Lett.* **66**, 3331 (1995).
- [21] V. Mujica, M. Kemp, and M. A. Ratner, *J. Chem. Phys.* **101**, 6849 (1994).
- [22] S. K. Maiti, *Solid State Commun.* **149**, 1684 (2009).
- [23] V. Mujica, M. Kemp, A. E. Roitberg, and M. A. Ratner, *J. Chem. Phys.* **104**, 7296 (1996).
- [24] S. K. Maiti, *Phys. Lett. A* **373**, 4470 (2009).
- [25] M. P. Samanta, W. Tian, S. Datta, J. I. Henderson, and C. P. Kubiak, *Phys. Rev. B* **53**, R7626 (1996).
- [26] S. K. Maiti, *J. Phys. Soc. Jpn.* **78**, 114602 (2009).
- [27] M. Hjort and S. Stafström, *Phys. Rev. B* **62**, 5245 (2000).
- [28] K. Walczak, *Cent. Eur. J. Chem.* **2**, 524 (2004).
- [29] K. Walczak, *Phys. Stat. Sol. (b)* **241**, 2555 (2004).
- [30] S. Datta, *Electronic transport in mesoscopic systems*, Cambridge University Press, Cambridge (1997).
- [31] M. B. Nardelli, *Phys. Rev. B* **60**, 7828 (1999).
- [32] O. Hod, R. Baer, and E. Rabani, *J. Phys. Chem. B* **108**, 14807 (2004).
- [33] O. Hod, R. Baer, and E. Rabani, *J. Phys.: Condens. Matter* **20**, 383201 (2008).
- [34] O. Hod, R. Baer, and E. Rabani, *J. Am. Chem. Soc.* **127**, 1648 (2005).
- [35] O. Hod, E. Rabani, and R. Baer, *Acc. Chem. Res.* **39**, 109 (2006).